# Supporting information

## Synergistic effect of electrolyte and intercalation engineering: comprehensive enhancement of electrochemical performance in a mixed proton–electron conducting layered vanadate cathode for aqueous zinc-ion batteries

Cheng Wang,[a] Ziqian Zeng,[a] Kefan Wang,[a] Dingjie Ma,[a] Yang Zou,[b] Qiao Qiao,[b] Zhiyuan Yao,[a,b,*] and Xiaoming Ren[b,c*]

[a] School of Physical and Mathematical Science, Nanjing Tech University, Nanjing 211816, P. R. China

[b] State Key Laboratory of Materials-Oriented Chemical Engineering and School of Chemistry and Molecular Engineering, Nanjing Tech University, Nanjing 211816, P. R. China

[c] State Key Laboratory of Coordination Chemistry, Nanjing University, Nanjing 210023, P. R. China

Email: zyyao@njtech.edu.cn (ZYY)

xmren@njtech.edu.cn (XMR)

**Contents**

Fig. S1 (a) The situation of the $\mathbf{C_4N_2}$**-VO** sample with water for three days. (b) TG plot of $\mathbf{C_4N_2}$**-VO** sample in 300–1073 K.

Fig. S2 Experimental and fitted impedance spectra of $\mathbf{C_4N_2}$**-VO** at the selected temperatures (Inset: the equivalent circuit).

Fig. S3 Experimental and fitted impedance spectra of $\mathbf{C_4N_2}$**-VO** at the selected temperatures (Inset: the equivalent circuit).

Fig. S4 Plots of $\sigma_{total}$ *vs.* $T$ of $\mathbf{C_4N_2}$**-VO**.

Fig. S5 (a) CV curves for the first ten cycles in the 0%-PEG electrolyte. (b) Charge-discharge curves at 0.2 A $g^{-1}$ of $\mathbf{C_4N_2}$**-VO** in the 0%-PEG electrolyte.

Fig. S6 Ragone plot of $\mathbf{C_4N_2}$**-VO** cathode in the 20%-PEG electrolyte.

Fig. S7 (a) CV curves at different scan rates under 0%-PEG electrolyte. (b) Log (*i*) *vs.* log (*v*) plot of four peaks in CV curves in the 0%-PEG electrolyte.

Table S1 The proton conductivity performance of common proton–conducting materials.

Table S2 The proton conductivity performance of water–assisted vanadium–based proton conductors.

Table S3 Comparison of the electrochemical performance of vanadium oxide–based cathode materials for AZIBs.

(a) (b)

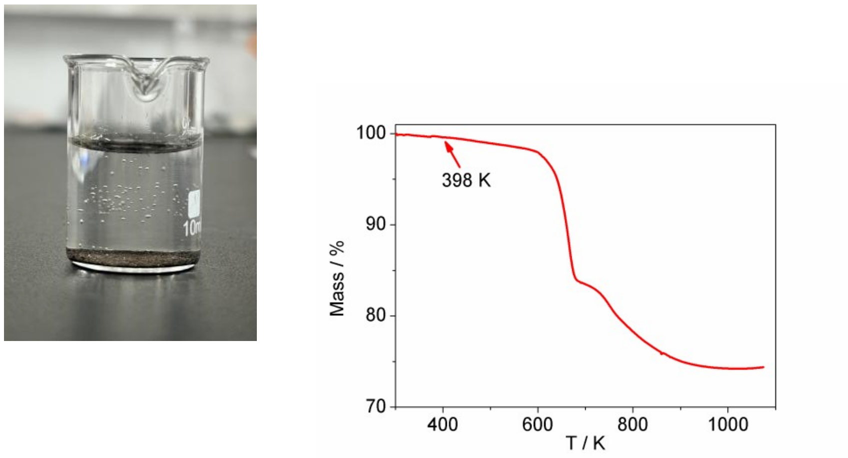


Fig. S1 (a) The situation of the **$C_4N_2$-VO** sample with water for three days. (b) TG plot of **$C_4N_2$-VO** sample in 300–1073 K.

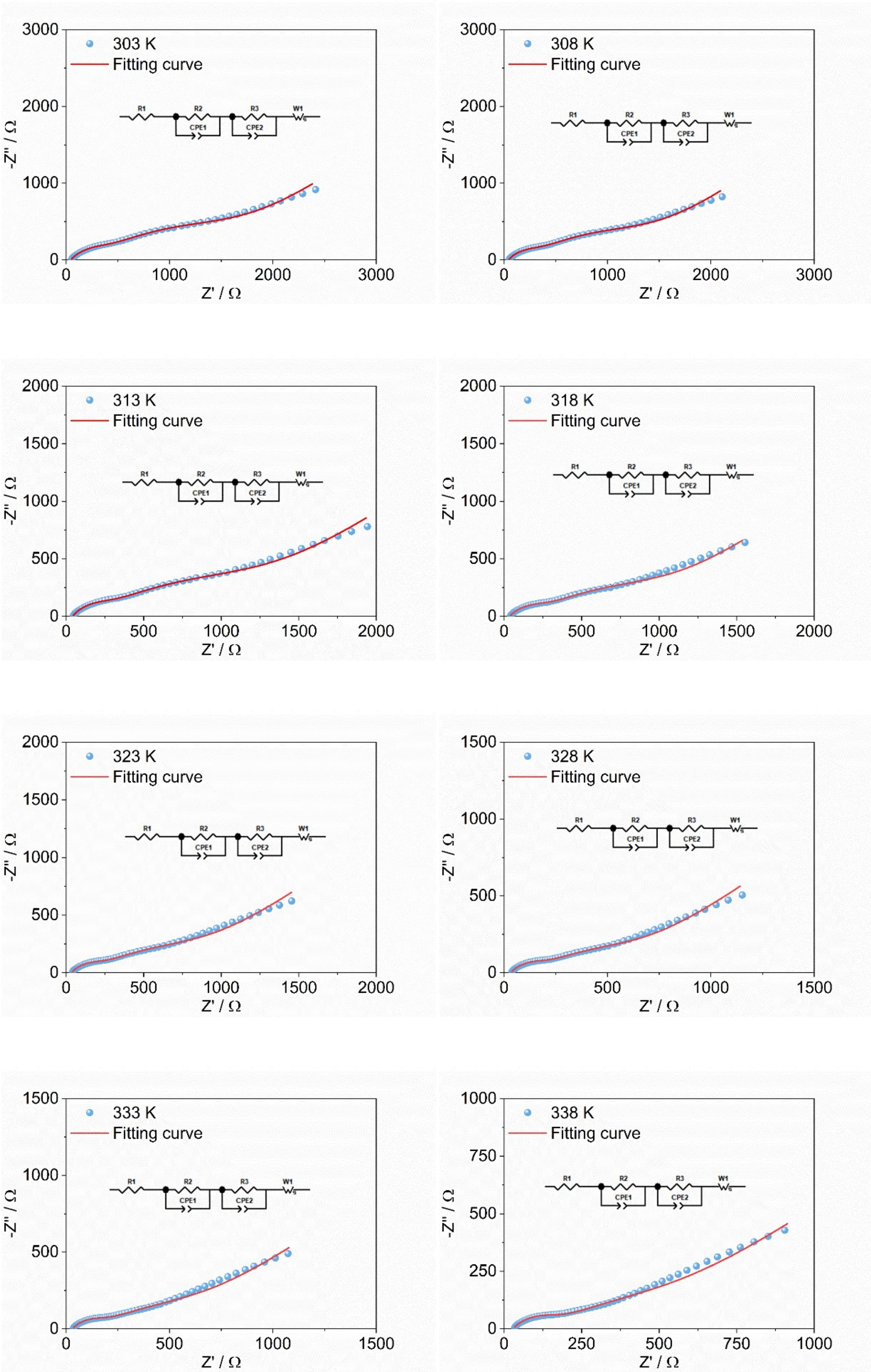


Fig. S2 Experimental and fitted impedance spectra of **$C_4N_2$-VO** at the selected temperatures (Inset: the equivalent circuit).

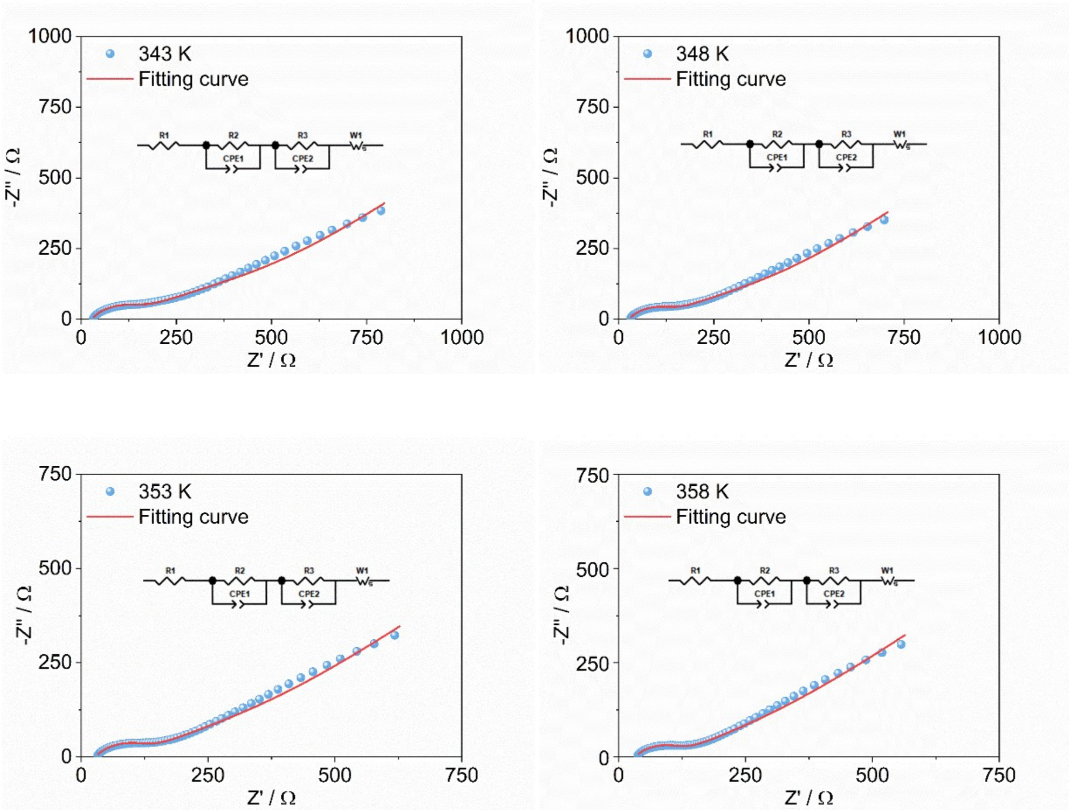


Fig. S3 Experimental and fitted impedance spectra of **$C_4N_2$-VO** at the selected temperatures (Inset: the equivalent circuit).

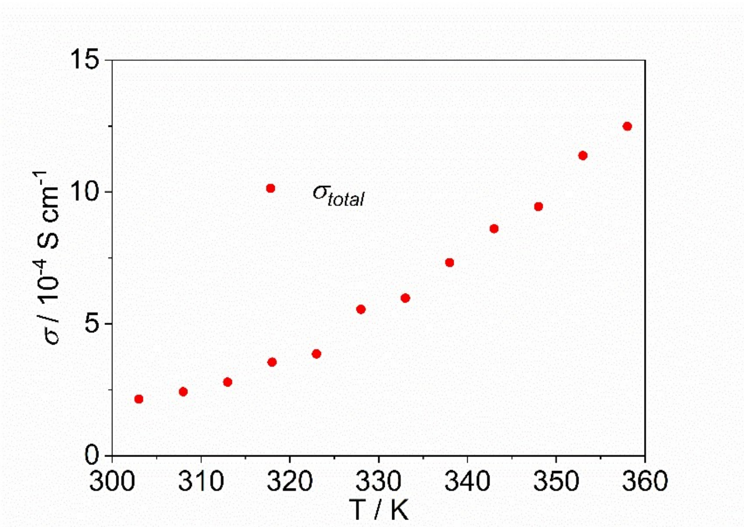


Fig. S4 Plots of $\sigma_{total}$ *vs.* $T$ of **$C_4N_2$-VO**.

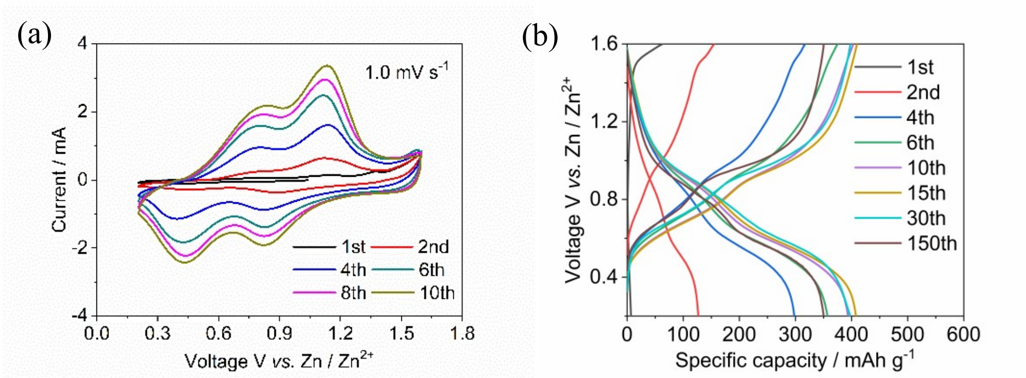


Fig. S5 (a) CV curves for the first ten cycles in the 0%-PEG electrolyte. (b) Charge-discharge curves at 0.2 A g$^{-1}$ of $\mathbf{C_4N_2}$**-VO** in the 0%-PEG electrolyte.

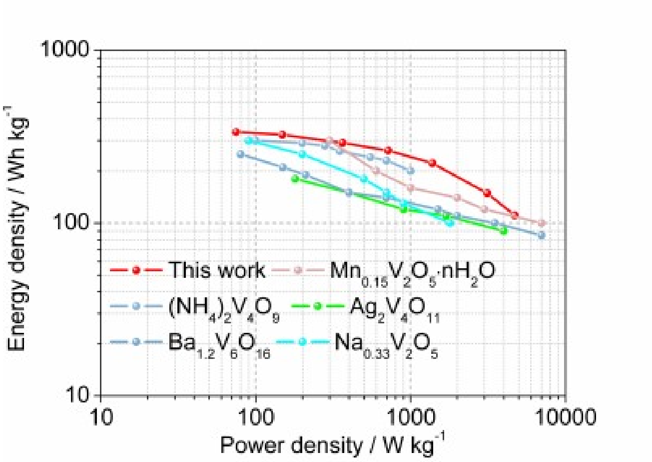


Fig. S6 Ragone plot of $\mathbf{C_4N_2}$**-VO** cathode in the 20%-PEG electrolyte.

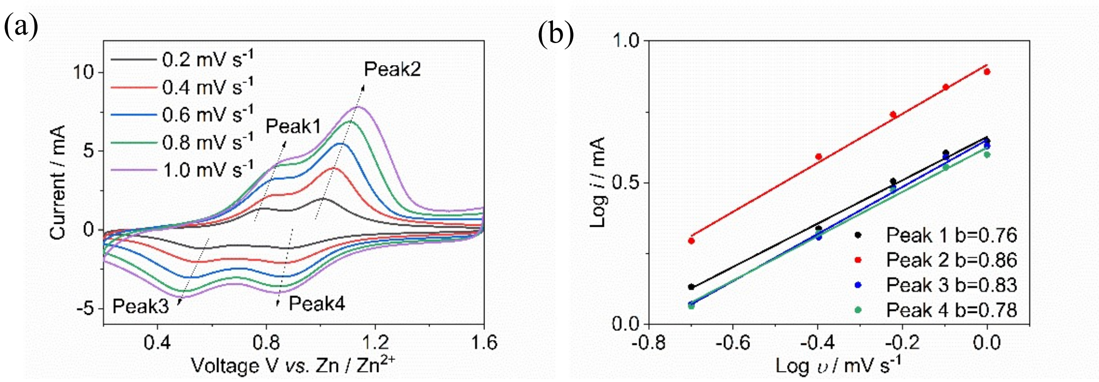


Fig. S7 (a) CV curves at different scan rates under 0%-PEG electrolyte. (b) Log (*i*) *vs.* log (*v*) plot of four peaks in CV curves in the 0%-PEG electrolyte.

Table S1 The proton conductivity performance of common proton–conducting materials.

| Compounds | Proton Conductivity ($S\cdot cm^{-1}$) | Temperature / humidity | Ref. |
|---|---|---|---|
| $\{[Zn-(C_{10}H_2O_8)_{0.5}(C_{10}S_2N_2H_8)]\cdot 2H_2O]\}_n$ | $4.39 \times 10^{-4}$ | 353 K / 98% RH | 1 |
| $(C_6N_4H_{22})_{0.5}[Zn(HPO_4)_2]$ | $4.60 \times 10^{-4}$ | 333 K / 98% RH | 2 |
| $Ni(HEDPH_3)_2(2,2'\text{-}Bipy)\cdot H_2O$ | $2.50 \times 10^{-3}$ | 363 K / 98% RH | 3 |
| PILP-OTF@MIL-101 | $7.61 \times 10^{-3}$ | 358 K / 98% RH | 4 |
| $(C_2N_2H_{10})_{0.5}CoPO_4$ | $2.05 \times 10^{-3}$ | 329 K / 98% RH | 5 |
| $(CH_3NH_3)_2Ag_4Sn_3S_8$ | $1.14 \times 10^{-3}$ | 340 K / 99% RH | 6 |
| MOF-801 | $1.88 \times 10^{-3}$ | 298 K / 98% RH | 7 |
| **$C_4N_2$-VO** | $1.18 \times 10^{-3}$ | 358 K / 98% RH | This work |

Table S2 The proton conductivity performance of water–assisted vanadium–based proton conductors.

| Compounds | $\sigma_{proton}$ ($S \cdot cm^{-1}$) | Temperature / Humidity | Ref. |
|---|---|---|---|
| $(C_6H_{14}N_2)[(VO)P_2O_7]$ | $3.30 \times 10^{-4}$ | 323 K / 100% RH | 8 |
| $V_2O_2(HPO_4)(HPO_3)(C_2O_4)_2 \cdot (C_4N_2H_{12})_2 \cdot 2H_2O$ | $4.35 \times 10^{-4}$ | 348 K / 98% RH | 9 |
| $Na_4[V_{12}B_{18}O_{54}(OH)_6(H_2O)] \cdot (H_2en)_4 \cdot 2(OH) \cdot 3H_2O$ | $2.55 \times 10^{-4}$ | 333 K / 100% RH | 10 |
| $[Ni(en)_3]_3 \cdot [1,3\text{-}dap]_2 \cdot H_6[V_{10}B_{26}O_{60}(OH)_{10}]$ | $1.78 \times 10^{-3}$ | 323 K / 100% RH | 11 |
| $K_2[(VO)_2(HPO_4)_2(C_2O_4)]$ | $1.15 \times 10^{-2}$ | 313 K / 95% RH | 12 |
| $[Cd(en)_2]_2[(V^{IV}O)_{10}(V^{V}O)_2B_{32}O_{66}(OH)_{18}(H_2O)_8] \cdot 14H_2O$ | $9.52 \times 10^{-4}$ | 358 K / 98% RH | 13 |
| **$C_4N_2$-VO** | $1.18 \times 10^{-3}$ | 358 K / 98% RH | This work |

Table S3 Comparison of the electrochemical performance of vanadium oxide–based cathode materials for AZIBs.

| Compounds | Specific capacity (mAh $g^{-1}$) | Operating conditions (V) | Capacity retention (loss / cycle) | Electrolyte | Ref. |
|---|---|---|---|---|---|
| MnVO | 415.0 (0.05 A $g^{-1}$) | 0.2 – 1.6 | 8% / 2000 (4 A $g^{-1}$) | 3 M $Zn(OTf)_2$ | 14 |
| $NH_4V_4O_{10}$ | 423.8 (0.1 A $g^{-1}$) | 0.5 – 1.7 | 13% / 2000 (2 A $g^{-1}$) | 3 M $Zn(OTf)_2$ | 15 |
| $Ba_{0.23}V_2O_5\cdot 1.1H_2O$ | 378 (0.1 A $g^{-1}$) | 0.3 – 1.6 | 7% / 2000 (5 A $g^{-1}$) | 3 M $Zn(OTf)_2$ | 16 |
| $Na_2V_6O_{16}\cdot 1.63H_2O$ | 352.0 (0.05 A $g^{-1}$) | 0.2 – 1.6 | 10% / 6000 (5 A $g^{-1}$) | 3 M $Zn(OTf)_2$ | 17 |
| $V_2O_5$ | 187.7 (1 A $g^{-1}$) | 0.4 – 1.4 | 11% / 180 (1 A $g^{-1}$) | 1 M $ZnSO_4$ with 20% PEG | 18 |
| $Na_{0.33}V_2O_5$ | 367.1 (0.1 A $g^{-1}$) | 0.2 – 1.6 | 7% / 1000 (1 A $g^{-1}$) | 3 M $Zn(OTf)_2$ | 19 |
| $(NH_4)_2V_4O_9$ | 376.0 (0.1 A $g^{-1}$) | 0.3 – 1.3 | 22% / 2000 (5 A $g^{-1}$) | 3 M $Zn(OTf)_2$ | 20 |
| $Ba_{1.2}V_6O_{16}\cdot 3H_2O$ | 345.5 (0.1 A $g^{-1}$) | 0.3 – 1.4 | 4% / 2000 (5 A $g^{-1}$) | 2 M $ZnSO_4$ | 21 |
| $HNaV_6O_{16}\cdot 4H_2O$ | 444.0 (0.5 A $g^{-1}$) | 0.2 – 1.6 | 6% / 1000 (5 A $g^{-1}$) | 3 M $Zn(OTf)_2$ | 22 |
| $Ag_2V_4O_{11}$ | 210.0 (0.2 A $g^{-1}$) | 0.4 – 1.7 | 7% / 6000 (5 A $g^{-1}$) | 3 M $Zn(OTf)_2$ | 23 |
| **$C_4N_2$-VO** | 382.4 (0.2 A $g^{-1}$) | 0.2 – 1.6 | 6% / 2000 (5 A $g^{-1}$) | 3 M $Zn(OTf)_2$ with 20% PEG | This work |

References


1 S. Sanda, S. Biswas and S. Konar, *Inorg. Chem.*, 2015, **54**, 1218–1222.

2 K. Zhang, M. Ji, X.Y. Zhou, F. Xuan, B. Duan, Y. Yuan, G. Liu, H. Duan and H. Zhao, *RSC Adv.*, 2023, **13**, 12703–12711.

3 I. Akhmetova, M. Rautenberg, C. Das, B. Bhattacharya and F. Emmerling, *ACS Omega*, 2023, **8**, 16687–16693.

4 S. Zhang, Y. Xie, R. J. Somerville, F. F. Tirani, R. Scopelliti, Z. Fei, D. Zhu and P. J. Dyson, *Small*, 2023, **19**, 2206999.

5 M. Wang, H.B. Luo, S.X. Liu, Y. Zou, Z.F. Tian, L. Li, J.L. Liu and X.M. Ren, *Dalton Trans.*, 2016, **45**, 19466–19472.

6 H.B. Luo, M. Wang, J. Zhang, Z.F. Tian, Y. Zou and X.M. Ren, *ACS Appl. Mater. Interfaces*, 2018, **10**, 2619–2627.

7 J. Zhang, H.J. Bai, Q. Ren, H.B. Luo, X.M. Ren, Z.F. Tian and S. Lu, *ACS Appl. Mater. Interfaces*, 2018, **10**, 28656–28663.

8 L. Zhang, C. Zhang, Y. Li, S. Xu, R. Liao, S. Zhang, S. Li and X. Liu, *Appl. Organomet. Chem.*, 2025, **39**, e70358.

9 Y. Yang, L. Huang, B. Li, S. Zhao, F. Zhang and Y. Bi, *Inorg. Chem. Commun.*, 2022, **141**, 109545.

10 X. Liu, B. Guo, L. Zhang, S. Zhao, Y. Dong and Z. Zhao, *New J. Chem.*, 2022, **46**, 16352–16358.

11 K. Bu, L. Zhang, F. Sun, D. Zeng, M. Jiang and H. Yuan, *Cryst. Growth Des.*, 2022, **22**, 1824–1830.

12 H.X. Sun, H.N. Wang, Y.H. Zou and X. Meng, *Inorg. Chem. Commun.*, 2021, **124**, 108322.

13 M.Z. Meng, B.L. Huang, S.S. Xu, Y.P. Chen and X.H. Huang, *Inorg. Chem.*, 2025,

**64**, 14287–14294.

14 C. Liu, Z. Neale, J. Zheng, X. Jia, J. Huang, M. Yan, M. Tian, M. Wang, J. Yang and G. Cao, *Energy Environ. Sci.*, 2019, **12**, 2273–2285.

15 K. Li, Y. Liu and X. Wu, *CrystEngComm*, 2022, **24**, 5421–5427.

16 X. Qin, Y. Du, P. Zhang, X. Wang, Q. Lu, A. Yang and J. Sun, *Int. J. Miner. Metall. Mater.*, 2021, **28**, 1684–1692.

17 P. Hu, T. Zhu, X. Wang, X. Wei, M. Yan, J. Li, W. Luo, W. Yang, W. Zhang, L. Zhou, Z. Zhou and L. Mai, *Nano Lett.*, 2018, **18**, 1758–1763.

18 X. Li, Y. Zhou, H. Tu, Z. Wang, R. Wu, Y. Lu, Y. Zong, Q. Liu, J. He, L. Qian, S. Song, Y. Zhang, C. Meng and A. Yuan, *J. Solid State Electrochem.*, 2024, **28**, 3209–3219.

19 P. He, G. Zhang, X. Liao, M. Yan, X. Xu, Q. An, J. Liu and L. Mai, *Adv. Energy Mater.*, 2018, **8**, 1702463.

20 Y. Zhang, H. Jiang, L. Xu, Z. Gao and C. Meng, *ACS Appl. Energy Mater.*, 2019, **2**, 7861–7869.

21 X. Wang, B. Xi, X. Ma, Z. Feng, Y. Jia, J. Feng, Y. Qian and S. Xiong, *Nano Lett.*, 2020, **20**, 2899–2906.

22 C. Guan, F. Hu, X. Yu, H. Chen, G. Song and K. Zhu, *Rare Met.*, 2022, **41**, 448–456.

23 Q. Li, Y. Liu, K. Ma, G. Yang and C. Wang, *Small Methods*, 2019, **3**, 1900637.